Chaotic memristive circuit: equivalent circuit realization and dynamical analysis*

Bao Bo-Cheng(包伯成)[a)†], Xu Jian-Ping(许建平)[b)], Zhou Guo-Hua(周国华)[b)], Ma Zheng-Hua(马正华)[a)], and Zou Ling(邹 凌)[a)]

[a)] *School of Information Science and Engineering, Changzhou University, Changzhou* 213164, *China*
[b)] *School of Electrical Engineering, Southwest Jiaotong University, Chengdu* 610031, *China*

(Received 8 June 2011; revised manuscript received 28 June 2011)

In this paper, a practical equivalent circuit of an active flux-controlled memristor characterized by smooth piecewise-quadratic nonlinearity is designed and an experimental chaotic memristive circuit is implemented. The chaotic memristive circuit has an equilibrium set and its stability is dependent on the initial state of the memristor. The initial state-dependent and the circuit parameter-dependent dynamics of the chaotic memristive circuit are investigated via phase portraits, bifurcation diagrams and Lyapunov exponents. Both experimental and simulation results validate the proposed equivalent circuit realization of the active flux-controlled memristor.

Keywords: chaos, dynamics, equivalent circuit, memristor

PACS: 05.45.–a **DOI:** 10.1088/1674-1056/20/12/120502

1. Introduction

A memristor is a two-terminal electronic device described by the nonlinear relation between i and v as $v = M(q)i$ or $i = W(\varphi)v$, where i, v, q, and φ are the current, the voltage, the charge and the flux of the device, respectively.[1,2] The memristance $M(q)$ and the memductance $W(\varphi)$ of the memristor[1] described by nonlinear functions $M(q) = \mathrm{d}\varphi(q)/\mathrm{d}q$ and $W(\varphi) = \mathrm{d}q(\varphi)/\mathrm{d}\varphi$ depend on how many electric charges and magnetic fluxes pass through the memristor in a particular direction, which means that the memristor has the distinctive ability to memorize the passed quantities of electric charges and magnetic fluxes. Therefore, appreciable research interest have been inspired by the successful fabrication of memristors because of their potential applications in computers, neural networks, analog circuitries, and so on.[3−7]

In the past three years, chaotic circuits with memristors have been investigated.[8−17] By replacing the active nonlinear resistance element, Chua's diode, in Chua's circuit with an active flux-controlled memristor, a four-dimensional memristor-based chaotic circuit was presented and novel features of chaotic behaviour were observed.[8−16] Several nonlinearities for characterizing the active flux-controlled memristors, such as non-smooth piecewise linearity,[8,9] smooth cubic nonlinearity,[10−14] smooth piecewise-quadratic nonlinearity,[15] etc., were used to emulate the relation between magnetic flux and electric charge. In Refs. [13] and [14], a circuit which possesses smooth cubic nonlinear characteristics is employed to realize the memristor-based chaotic circuit. Also, the fractional-order memristor-based Chua's circuit and the simplest memristor-based chaotic circuit were recently presented in Refs. [16] and [17]. Apart from the interesting fundamental studies of nonlinear systems, the field of applications of such circuits includes secure communications with chaos.[9]

Recently, much attention has been paid to such memristor-based chaotic circuits and their dynamical analyses. However, the design of the circuit, in which the properties of these memristors characterized by numerous nonlinearities[8−16] are used, requires extensive simulation and experimental verification.[13,14] Thus, an equivalent circuit model is desirable to realize a memristor.[18,19] Such a model must take into account the physical properties of the memristor which lead to its nonlinear and hysteretic behaviours.[6,20] In this paper, a practical equivalent circuit is presented, which captures the behaviour of an active flux-controlled memristor with smooth piecewise-quadratic nonlinearity.[15] Based on the equivalent circuit, a chaotic memristive circuit is implemented

*Project supported by the Natural Science Foundation of Jiangsu Province of China (Grant No. BK2009105).
†Corresponding author. E-mail: mervinbao@126.com
© 2011 Chinese Physical Society and IOP Publishing Ltd

and its strange attractor is experimentally observed. Furthermore, the initial state-dependent and circuit parameter-dependent dynamics of the chaotic memristive circuit are investigated.

2. Equivalent circuit realization of a memristor

2.1. Active flux-controlled memristor

In this paper, an active memristor is characterized by smooth piecewise-quadratic nonlinearity as[15]

$$q(\varphi) = -a\varphi + 0.5b\varphi^2 \mathrm{sgn}(\varphi), \tag{1}$$

where a and b are both positive real constants and $\mathrm{sgn}(\cdot)$ is the sign function. Thus, its corresponding memductance, $W(\varphi)$, can be given as

$$W(\varphi) = \mathrm{d}q(\varphi)/\mathrm{d}\varphi = -a + b\,|\varphi|\,. \tag{2}$$

Since the memductance $W(\varphi)$ may become negative in certain working ranges, the power $p(t) = W(\varphi)v(t)^2$ and the energy $w(t_0, t) = \int_{t_0}^{t} p(\tau)\,\mathrm{d}\tau$ (for all $t \geq t_0$) will vary between positive and negative with the time evolution. Thus, the memristor constitutive relation is active. An active memristor can be equivalent to a memristive circuit consisting of a passive memristor with a negative resistor.[1,8,20]

2.2. Equivalent circuit realization

The circuit schematic diagram to realize the memristor characterized by Eq. (1) is shown in Fig. 1, where $H(\cdot)$ is a circuit characterized by nonlinear function. The operational amplifier U_1 is used to avoid loading effects.[13] The operational amplifier U_2 connecting with the resistor R and capacitor C is an integrator, which realizes the relationship as

$$v_{\mathrm{a}}(t) = -\frac{1}{R_0 C_0}\int_{-\infty}^{t} v(t)\,\mathrm{d}\tau = -\xi\varphi(t), \tag{3}$$

where $\varphi(t) = \int_{-\infty}^{t} v(t)\,\mathrm{d}\tau$, and $\xi = 1/R_0C_0$.

From Fig. 1(a), the output of the multiplier M_1 is given as

$$v_{\mathrm{c}}(t) = g_1 H[v_{\mathrm{a}}(t)]v(t), \tag{4}$$

where g_1 is a variable scale factor in the multiplier M_1. The operational amplifier U_3 in Fig. 1(a) is the current–inverter that implements[13] (when $R_2 = R_3$)

$$i(t) = \left\{\frac{-1}{R_1} + \frac{g_1 H[v_{\mathrm{a}}(t)]}{R_1}\right\} v(t). \tag{5}$$

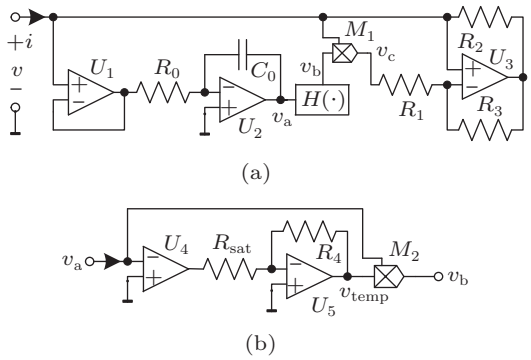


Fig. 1. Equivalent circuit of memristor with smooth piecewise-quadratic nonlinearity: (a) main circuit; (b) $H(\cdot)$ circuit with absolute value nonlinearity.

Figure 1(b) depicts that the circuit with absolute value nonlinearity $H(\cdot)$ is realized by a circuit consisting of one multiplier, two operational amplifiers and two resistors. In Fig. 1(b), there exists

$$v_{\mathrm{b}}(t) = H[v_{\mathrm{a}}(t)] = \frac{g_2 R_4 E_{\mathrm{sat}}}{R_{\mathrm{sat}}}\,|v_{\mathrm{a}}(t)|\,, \tag{6}$$

where g_2 is a variable scale factor in the multiplier M_2 and E_{sat} is the saturated output voltage of operational amplifier.

Then substituting Eqs. (3) and (6) into Eq. (5), we obtain the expression of the equivalent memductance in Fig. 1 as

$$W(\varphi) = \frac{-1}{R_1} + \frac{g_1 g_2 R_4 E_{\mathrm{sat}}\xi}{R_1 R_{\mathrm{sat}}}\,|\varphi|\,. \tag{7}$$

Using the definitions of the flux across and the current through a flux-controlled memristor along with the memductance given above, we have

$$\varphi(t) = \int_{-\infty}^{t} v(t)\,\mathrm{d}\tau,\ \ i(t) = (-a + b\,|\varphi|)\,v(t). \tag{8}$$

Comparing Eqs. (3), (5), and (8) we can see that the equivalent circuit in Fig. 1 does realize an active flux-controlled memristor. Also, comparing Eq. (2) and Eq. (7) we have the following relationships:

$$a = \frac{1}{R_1},\ \ b = \frac{g_1 g_2 R_4 E_{\mathrm{sat}}\xi}{R_1 R_{\mathrm{sat}}}. \tag{9}$$

2.3. Simulation results of memristor

In our equivalent circuit implementation of an active flux-controlled memristor, the circuit parameters are listed in Table 1, with AD633JN as analog multiplier, AD711kN as operational amplifier, and an operation voltage of ±15 V. Then we can obtain the equivalent parameters of the proposed active flux-controlled memristor as: $a = 0.6667$ mS and $b = 1.4828$ S/Wb. The PSpice simulation results of the $v(t)$–$i(t)$ curves of this memristor with a periodic input under amplitude 2 V and frequency 1000 Hz are depicted in

Fig. 2(a). Note that the memristor typically behaves as a pinched hysteresis loop characteristic, namely there may be at most two values of the current $i(t)$ for a given voltage $v(t)$. The corresponding Matlab simulation results of the $v(t)$–$i(t)$ curves based on model (2) with the same stimulus are displayed in Fig. 2(b). Note that two curves are consistent with each other.

Table 1. Circuit parameters of a memristor equivalent circuit.

Circuit parameters	Values
Capacitor C_0	68 nF
Resistor R_0	4 kΩ
Resistor R_1	1.5 kΩ
Resistors R_2, R_3	2 kΩ, 2 kΩ
Resistor R_4	6.05 kΩ
Resistor $R_{\rm sat}$	13.5 kΩ
Scale factor $(M_1)g_1$	0.1
Scale factor $(M_2)g_2$	1

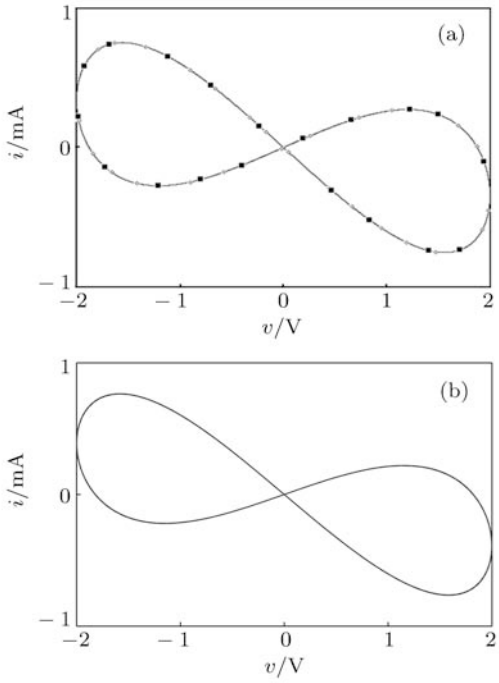


Fig. 2. Current–voltage curves of a pinched hysteresis loop of the memritor with a periodic stimulus: (a) PSpice simulation; (b) Matlab simulation.

3. Chaotic memristive circuit and results

3.1. Chaotic memristive circuit

Figure 3 shows a chaotic circuit with an active memristor, which is directly extended from Chua's circuit by replacing the Chua diode with the flux-controlled memristor.[8−16] The flux-controlled memristor is an active two-terminal electronic device described by Eq. (1). The equations for the chaotic memristive circuit can be written as

$$\begin{cases} \dfrac{{\rm d}v_1}{{\rm d}t} = \dfrac{1}{C_1}\left(\dfrac{v_2 - v_1}{R} - W(\varphi)v_1\right), \\ \dfrac{{\rm d}v_2}{{\rm d}t} = \dfrac{1}{C_2}\left(\dfrac{v_1 - v_2}{R} - i_3\right), \\ \dfrac{{\rm d}i_3}{{\rm d}t} = \dfrac{1}{L}\left(v_2 - ri_3\right), \\ \dfrac{{\rm d}\varphi}{{\rm d}t} = v_1, \end{cases} \tag{10}$$

where $\varphi(t)$ denotes the magnetic flux between two terminals of a memristor.

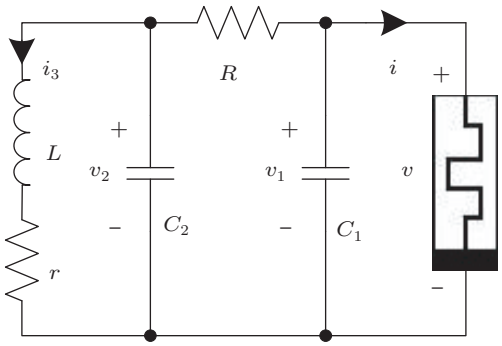


Fig. 3. Chaotic memristive circuit.

3.2. Simulation results

The values of circuit parameters are shown in Table 2 and the initial values of state variables are $v_1(0) = 10^{-10}$ V, $v_2(0) = 0$ V, $i_3(0) = 0$ A, and $\varphi(0) = 0$ Wb. Figure 4 displays the strange attractors of the chaotic memristive circuit. Making use of Wolf's method to calculate Lyapunov exponents,[21] the results are (545.1359, 0, −377.4216, −7195.5943), from which we can see clearly that the system is in a chaotic state.

Table 2. Circuit parameters of memristor-based chaotic circuit.

Circuit parameters	Values
Inductor L	17.2 mH
Capacitor C_1	6.8 nF
Capacitor C_2	68 nF
Resistor R	2.1 kΩ
Resistor r	2 Ω
Memristor a, b	0.6667 mS, 1.4828 S/Wb

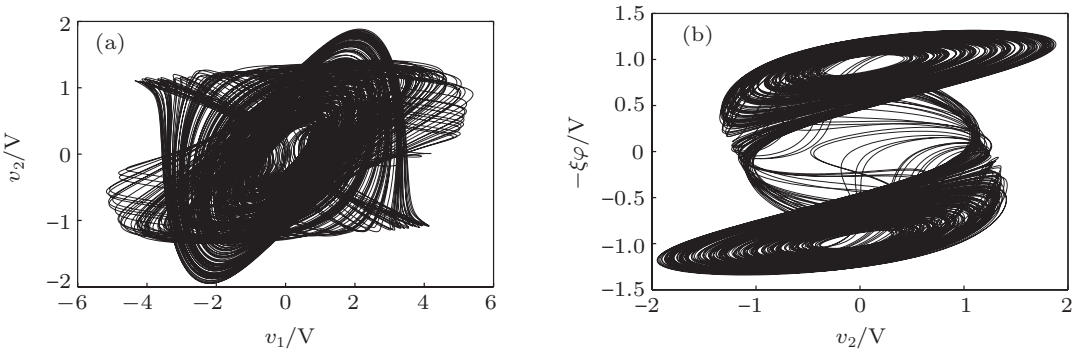


Fig. 4. Numerical phase portraits of the chaotic attractor: (a) $v_1$versus v_2; (b) v_2 versus $-\xi\phi$.

3.3. Experiment results

Based on the schematics in Figs. 1 and 3, an experimental prototype of the chaotic memristive circuit with memristor equivalent circuit is built. The parameters of experimental setup are given in Tables 1 and 2. The experimental observations are shown in Fig. 5, which reveal that the circuit exhibits chaotic behaviour. These results are in good agreement with simulations.

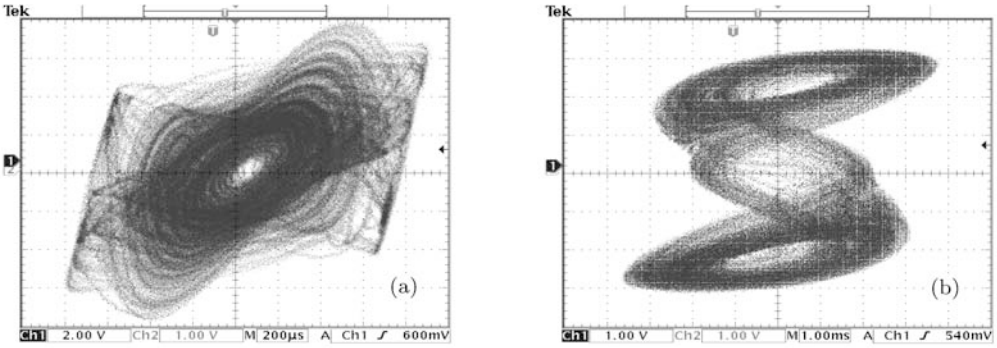


Fig. 5. Measured phase portraits of the chaotic attractor: (a) $v_1$versus v_2; (b) v_2 versus $v_{\rm a}$.

4. Dynamics of the chaotic memristive circuit

4.1. Equilibrium point and stability

The equilibrium points of Eq. (10) can be found by setting the left-hand side to be zero. Obviously,

$$E = \{(v_1, v_2, i_3, \varphi)\,|v_1 = v_2 = i_3 = 0, \varphi = \varphi_0\} \quad (11)$$

is one equilibrium of the system, where φ_0 is uncertain but constant.[14] The Jacobian matrix of system (10) can be described as

$$\boldsymbol{J} = \begin{bmatrix} -\dfrac{1+R(a+b\,|\varphi|)}{RC_1} & \dfrac{1}{RC_1} & 0 & -\dfrac{bv_1\mathrm{sgn}(\varphi)}{C_1} \\ \dfrac{1}{RC_2} & -\dfrac{1}{RC_2} & -\dfrac{1}{C_2} & 0 \\ 0 & \dfrac{1}{L} & -\dfrac{r}{L} & 0 \\ 1 & 0 & 0 & 0 \end{bmatrix}. \quad (12)$$

At equilibrium point E, the system characteristic equation can be written as

$$\lambda(\lambda^3 + a_2\lambda^2 + a_1\lambda + a_0) = 0, \quad (13)$$

where

$$a_2 = \frac{1}{RC_1} + \frac{1}{RC_2} + \frac{a+b|\varphi_0|}{C_1} + \frac{r}{L},$$
$$a_1 = \frac{a+b|\varphi_0|}{C_1}\Big(\frac{1}{RC_2} + \frac{r}{L}\Big) + \frac{1}{LC_2} + \frac{r}{RL}\Big(\frac{1}{C_1} + \frac{1}{C_2}\Big),$$
$$a_0 = \frac{1}{RLC_1C_2} + \frac{a+b|\varphi_0|}{LC_1C_2}\Big(1 + \frac{r}{R}\Big).$$

E is defined as an unstable equilibrium when at least one root of Eq. (13) has the real part greater than zero. Apparently, the coefficients of the cubic polynomial inside brackets of Eq. (13) are all nonzero. Taking advantage of the values of system parameters shown in Table 2 and Routh–Hurwitz condition, one or more roots of this cubic polynomial equation have positive real parts when

$$\begin{cases} |\varphi_0| < 0.1288 \text{ mWb or} \\ 0.1596 \text{ mWb} < |\varphi_0| < 0.3805 \text{ mWb}. \end{cases} \quad (14)$$

Equation (14) demonstrates that the dynamical behaviours of this chaotic memristor circuit are determined by the initial state of the variable $\varphi(t)$.[10,14,15] System (10) is unstable when φ_0 satisfies condition (14).

Three nonzero eigenvalues λ_i $(i = 1, 2, 3)$ of the equilibrium point E for some typical values of the constant φ_0 are listed in Table 3, which are characterized by an unstable or stable saddle-focus. Thus, the dynamical behaviours of the chaotic memristive circuit are closely dependent on the initial state of the state variable $\varphi(t)$. Such characteristics well reflect the unique properties of memristor element.

Table 3. Three nonzero eigenvalues λ_i $(i = 1, 2, 3)$ of the equilibrium point.

φ_0/mWb	λ_1	$\lambda_{2,3}$
0	35388.5856	$-7248.2306 \pm$ j25029.4548
0.1	11541.7772	$-6228.0848 \pm$ j20645.1163
0.12876	0	$-3592.855 \pm$ j18787.787
0.14	−5809.4843	$-1913.7574 \pm$ j18906.1396
0.15960	−13912.0655	±j20341.4604
0.2	−24965.8555	$1122.4732 \pm$ j23049.3587
0.38054	−62091.2275	±j27509.3862
0.5	−86506.7046	$-816.8774 \pm$ j28288.0695

4.2. Initial state-dependent dynamics

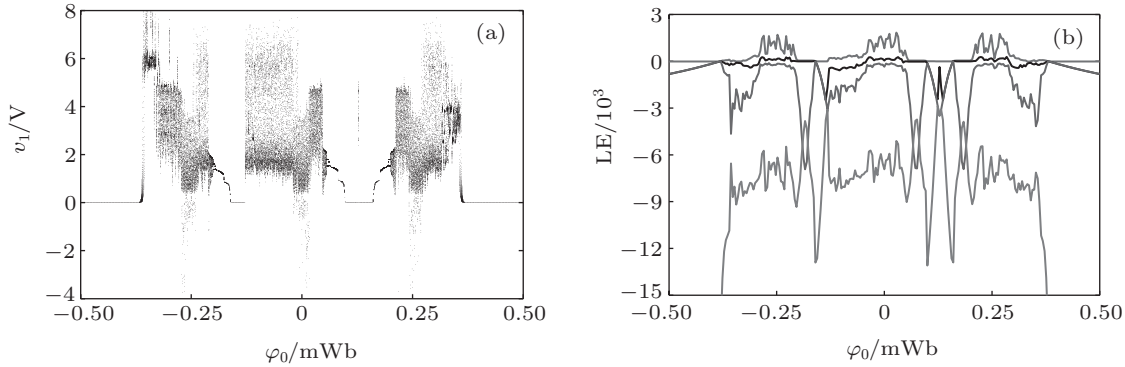


Fig. 6. Dynamical behaviours with the variation of the initial state φ_0: (a) bifurcation diagram; (b) Lyapunov exponents.

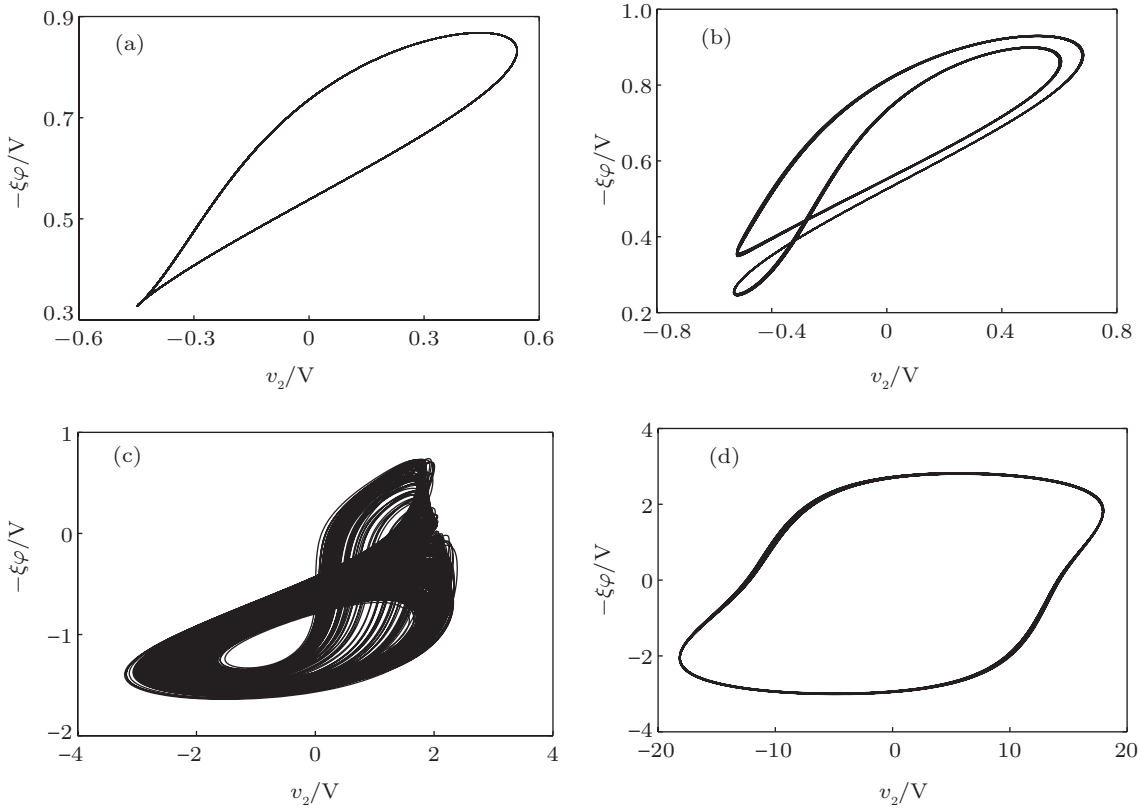


Fig. 7. Typical orbits in memristive circuit: (a) period-1 ($\varphi_0 = -0.19$ mWb); (b) period-2 ($\varphi_0 = -0.2$ mWb); (c) 1-scroll attractor ($\varphi_0 = -0.1$ mWb); (d) period-1 ($\varphi_0 = 0.37$ mWb).

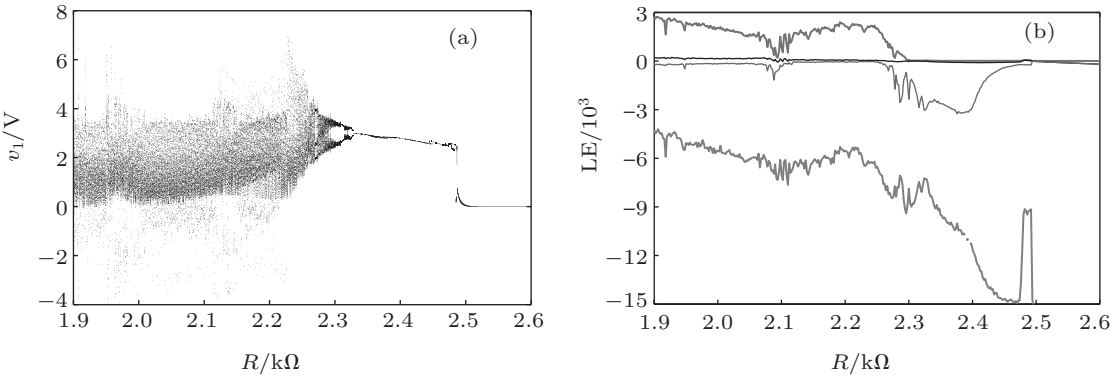


Fig. 8. Dynamical behaviours of memristive circuit with R increasing: (a) bifurcation diagram; (b) Lyapunov exponents.

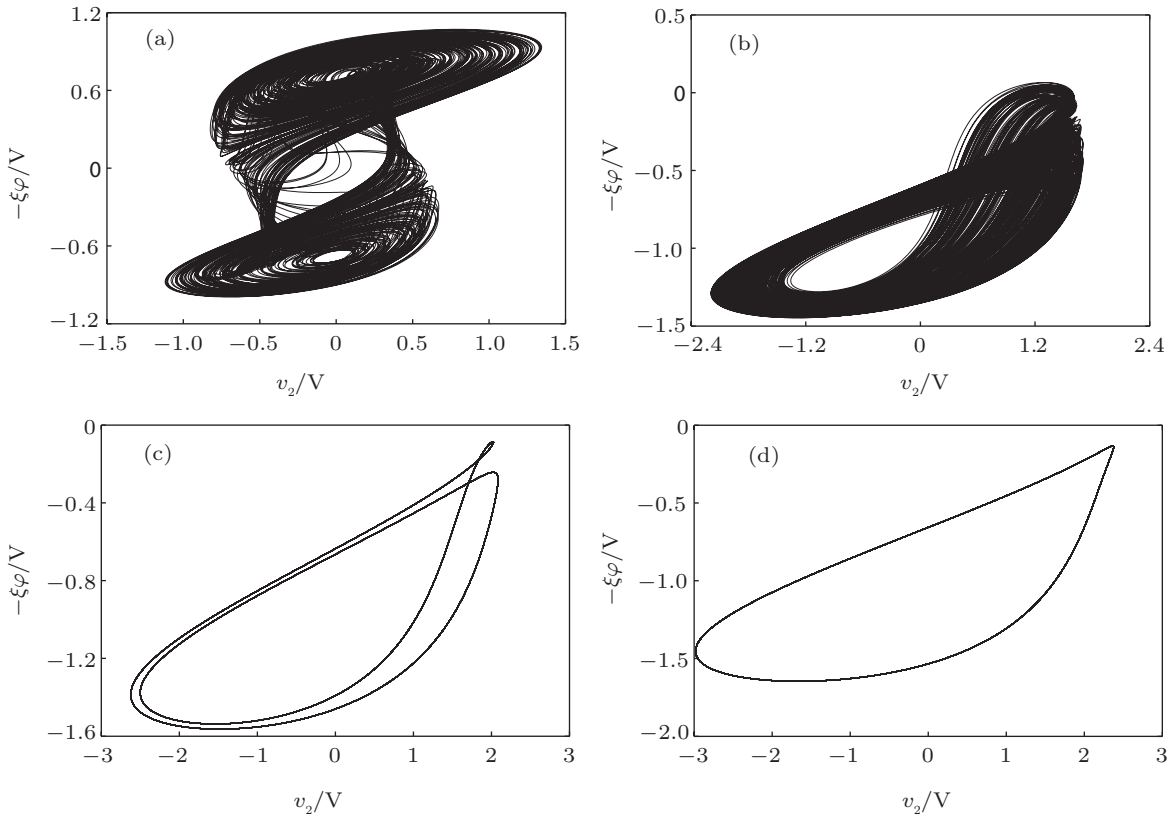


Fig. 9. Typical orbits in memristive circuit: (a) 2-scroll attractor ($R = 1.9$ kΩ); (b) 1-scroll attractor ($R = 2.25$ kΩ); (c) period-2 ($R = 2.31$ kΩ); (d) period-1 ($R = 2.33$ kΩ).

For the above circuit parameters, the initial state φ_0 is a varying parameter. When the initial state φ_0 increases gradually, the bifurcation diagram of state variable $v_1(t)$ and the corresponding Lyapunov exponent spectra are depicted in Figs. 6(a) and 6(b), respectively. Note that the Poincaré section $v_2(t) = 0$ V is selected to plot the bifurcation diagram. It is seen that the bifurcation diagram well coincides with the Lyapunov exponent spectra. Observed from Fig. 6, system (10) has abundant and complex dynamical behaviours. In three regions $[-0.35, -0.21]$, $[-0.12, 0.05]$, and $[0.21, 0.35]$ of the initial state φ_0, system (10) is chaotic with different undergoing chaotic routes observed from Fig. 6(a) and with a positive Lyapunov exponent, two zero Lyapunov exponents along with a negative Lyapunov exponent observed from Fig. 6(b). As φ_0 increases, Hopf and period-doubling bifurcation routes to chaos exist in the chaotic memristive circuit. Consequently, the numerical simulation results of the initial state-dependent dynamical behaviours, are consistent with those from theoretical analyses.

Some typical orbits of system (10) are obtained from numerical simulations as shown in Fig. 7. Figures 7(a) and 7(b) show two limit cycles with period 1 and period 2 separately, and figure 7(c) illustrates a 1-scroll chaotic attractor, and Fig. 7(d) exhibits a limit

cycle of period 1 with bigger dynamic amplitude. Observed from Fig. 7, there exhibit great variations of the orbits of system (10) under different initial values. Therefore, it is remarkable that compared with conventional chaotic system,[22−31] the chaotic memristive circuit has more complicated routes to chaos, depending on initial states.

4.3. Circuit parameter dependent dynamics

For simplicity, only a special condition $\phi_0 = 0$ Wb is taken into account here.[14] Under the variation of resistance R, the bifurcation diagram of the state variable $v_1(t)$ of system (10) and the corresponding Lyapunov exponent spectra are shown in Figs. 8(a) and 8(b), respectively. Figure 8(a) shows clearly that the output voltage settles first in period-1 steady state and then goes to chaotic oscillation through period-doubling bifurcation with resistance R decreasing gradually. In particular, a narrow periodic window appears near 2.094 kΩ, where the maximum Lyapunov exponent tends to zero. The periodic window plays an important role in the transition from chaotic to hyperchaotic behaviour. Some typical orbits of system (10) are obtained from numerical simulations as shown in Fig. 9. Figure 9(a) shows a 2-scroll hyperchaotic attractor, figure 9(b) depicts a 1-scrpll chaotic attractor, figure 9(c) displays a limit cycle with period-2, and figure 9(d) exhibits a limit cycle with period-1.

5. Conclusion

In this paper, we present a practical equivalent circuit of an active flux-controlled memristor characterized by smooth piecewise-quadratic nonlinearity and an experiment set-up of a chaotic memristive circuit. Furthermore, we investigate the dynamics of the chaotic memristive circuit with the help of nonlinear tools.

The experimental results show that the equivalent circuit presented in this paper provides a practical memristor implementation. Based on the equivalent circuit of memristor, the chaotic memristive circuit can be easily designed and experimentally observed. The equilibrium point stability analysis indicates that the stability of the chaotic memristive circuit is closely dependent on the initial state of the memristor, which makes its dynamical behaviours more complicated, completely different from the existing chaotic system. Typical periodic and chaotic trajectories dependent on initial states and circuit parameters of the chaotic memristive circuit are shown and the Lyapunov exponents and the bifurcation diagrams are investigated to confirm the emergence of chaos.

References

[1] Chua L O 1971 *IEEE Trans. Circ. Theory* **CT-18** 507
[2] Strukov D B, Snider G S, Stewart D R and Williams R S 2008 *Nature* **453** 80
[3] Wang F Z, Helian N, Wu S, Lim M G, Guo Y and Parker M A 2010 *IEEE Electron. Dev. Lett.* **31** 755
[4] Pershin Y V and Di Ventra M 2010 *Neural Networks* **23** 881
[5] Pershin Y V and Di Ventra M 2010 *IEEE Trans. Circuits Sys.* I: *Regular Papers* **57** 1857
[6] Pershin Y V and Di Ventra M 2011 *Adv. Phys.* **60** 145
[7] Witrisal K 2009 *Electron. Lett.* **45** 713
[8] Itoh M and Chua L O 2008 *Int. J. Bifurc. Chaos* **18** 3183
[9] Muthuswamy B and Kokate P P 2009 *IETE Tech. Rev.* **26** 415
[10] Bao B C, Liu Z and Xu J P 2010 *Electron. Lett.* **46** 228
[11] Bao B C, Liu Z and Xu J P 2010 *Chin. Phys.* B **19** 030510
[12] Bao B C, Liu Z and Xu J P 2010 *Acta Phys. Sin.* **59** 3785 (in Chinese)
[13] Muthuswamy B 2010 *Int. J. Bifurc. Chaos* **20** 1335
[14] Iu H H C, Yu D S, Fitch A L, Sreeram V and Chen H 2011 *IEEE Trans. Circuits Sys. I*: *Regular Papers*, DOI: 10.1109/TCSI.2010. 2097771
[15] Bao B C, Xu J P and Liu Z 2010 *Chin. Phys. Lett.* **27** 070504
[16] Petráš I 2010 *IEEE Trans. Circuits Sys.* II: *Exp. Briefs* **57** 975
[17] Muthuswamy B and Chua L O 2010 *Int. J. Bifurc. Chaos* **20** 1567
[18] Pershin Y V and Di Ventra M 2010 *Electron. Lett.* **46** 517
[19] Biolek D and Biolková V 2010 *Electron. Lett.* **46** 1428
[20] Riaza R 2010 *IEEE Trans. Circuits Sys.* II: *Exp. Briefs* **57** 223
[21] Wolf A, Swift J, Swinney H and Vastano J 1985 *Physica* D: *Nonlinear Phenomena* **16** 285
[22] Bao B C, Liu Z and Yu J B 2009 *Int. J. Bifurc. Chaos* **19** 2573
[23] Liu L, Su Y C and Liu C X 2007 *Chin. Phys.* **16** 1897
[24] Bao B C, Li C B, Xu J P and Liu Z 2008 *Chin. Phys.* B **17** 4022
[25] Dong E N, Chen Z P, Chen Z Q and Yuan Z Z 2009 *Chin. Phys.* B **18** 2680
[26] Li C B and Wang D C 2009 *Acta Phys. Sin.* **58** 764 (in Chinese)
[27] Liu C X and Liu L 2009 *Chin. Phys.* B **18** 2188
[28] Dai H, Jia L X, Hui M and Si G Q 2011 *Chin. Phys.* B **20** 040507
[29] Zhang Y and Bi Q S 2011 *Chin. Phys.* B **20** 010504
[30] Sun K H, Yang J L, Ding J F and Sheng L Y 2010 *Acta Phys. Sin.* **59** 8385 (in Chinese)
[31] Feng C W, Cai L, Zhang L S, Yang X K and Zhao X H 2010 *Acta Phys. Sin.* **59** 8426 (in Chinese)